NCU Data Paper for LEAP-ASIA-2019

Jun-Xue Huang[1], Truong-Nhat-Phuong Pham[1], Wen-Yi Hung[2]

[1]*Ph.D. Student, Department of Civil Engineering, National Central University, Taiwan*

[2]*Associate Professor, Department of Civil Engineering, National Central University, Taiwan*

1. Brief description of the experiments

Two tests for LEAP-ASIA-2019 were conducted at National Central University (NCU) and the testing conditions are listed at Table 1-1. The dimensions of model are 767 mm (L) × 355 mm (W) × 153.8 mm (H) with 1643 kg/m^3 (model A) and 1626 kg/m^3 (model B) of dry unit weight by using Ottawa F-65 sand. A 5-degree slope and curvature ground surface are the same as the models of LEAP-UCD-2017. The centrifuge modeling factor, η, are 26 and 13; and the virtual 1 g modeling scaling factor, μ, are 1 and 2 for model A and B, respectively. Therefore, models A and B were carried out under 26 g and 13 g acceleration field. The scaling factors of physical quantities adopted in NCU tests are listed in Table 1-2.

During spinning, total 3 shaking events were applied including one destructive and two nondestructive motions. The destructive 16-cycle tapered sine wave was 1 Hz frequency and target effective peak base acceleration (PBA_{eff}) of about 0.1 g. Before and after destructive motion, two nondestructive motions with 3 Hz frequency and 0.04 g amplitude of 1-cycle sine wave were input to detect the shear velocity and predominant frequency of soil strata. The characteristics of shaking events are listed in Table 1-3. The achieved PBA_{eff} of destructive motions are 0.141 g and 0.126 g for models A and B, respectively.

The models were prepared and following the test procedure of LEAP-UCD-2017, as shown in Figure 1-1. The sand bed was made by air-pluviation method with a constant drop height of 500 mm and flow rate of 2.5 kg/min. The accelerometers and pore pressure transducers were installed at a specific location during pluviating. The 5 degrees slope and curved surface were formed by using a vacuum and a specific curved acrylic scraper after air-pluviation completed. 18 PVC surface markers were then placed and 12 sticks of spaghetti were penetrated vertically into soil strata at the certain locations.

Pure CO_2 was filled from the bottom of the container for 1.5 hours with air flow rate of 0.25 kg/cm^2 to replace the air in the container before saturation. The methylcellulose solution with specific viscosity was dropped on the sponge putting on the slope surface to saturate model with a flow rate of 1 kg/hour under stable vacuum pressure. The degree of saturation was measured by Okamura method and it should be higher than 99.5%. Then the location and elevation of markers were measured by using digital vernier caliper.

NCU centrifuge was spinning from 1 g to certain g-level (26 g for model A and 13 g for model B), and the tests were carried out by the sequence described below; (1) the first shaking event, a nondestructive motion, was inputted; (2) the first CPT test was implemented; (3) second shaking event, a destructive motion, was input; (4) the second CPT test was implemented; (5) the third shaking event, a nondestructive motion, was input. After testing, the centrifuge was stopped to measure the final location and elevation of makers and cut the soil profile to observe deformation behavior of spaghetti and the position of pore pressure transducers at the middle array.

Table 1-1 Conditions of models

Test No.	Scaling factor		Achieve density	PBA	PBA_{eff}	PBA_{1Hz}
	Centrifuge, η	Virtual 1g, μ	(kg/m^3)	(g)	(g)	(g)
Model A	26	1	1643	0.180	0.141	0.108
Model B	13	2	1628	0.164	0.126	0.096

Table 1-2 Scaling factors adopted for NCU models

Physical quantity	Generalized scaling factor	Model A	Model B
Length	$\mu\eta$	26	26
Density	1	1	1
Time	$\mu^{0.75}\eta$	26	21.8
Frequency	$\mu^{-0.75}/\eta$	1/26	1/21.8
Acceleration	$1/\eta$	1/26	1/13
Velocity	$\mu^{0.75}$	1	1.68
Displacement	$\mu^{1.5}\eta$	26	36.8
Stress	μ	1	2
Strain	$\mu^{0.5}$	1	1.41
Stiffness	$\mu^{0.5}$	1	1.41
Permeability	$\mu^{0.75}\eta$	26	21.8
Pore pressure	μ	1	2

Table 1-3 Characteristics of three shaking events

Event No.	Frequency (Hz)	PBA (model A / model B)	Cycle	Type
s1	3	0.036 g / 0.045 g	1	Pre-shaking (nondestructive) Rectangular sine wave
s2	1	0.180 g / 0.164 g	16	Main shaking (destructive) Tapered sine wave
s3	3	0.035 g / 0.046g	1	Pre-shaking (nondestructive) Rectangular sine wave

Finally, the achieved PBA_{eff} of destructive motions are 0.112 g and 0.104 g in model A and B, respectively.

Figure 1-1. The procedure of LEAP tests at National Central University.

2. Before and after photos of tests

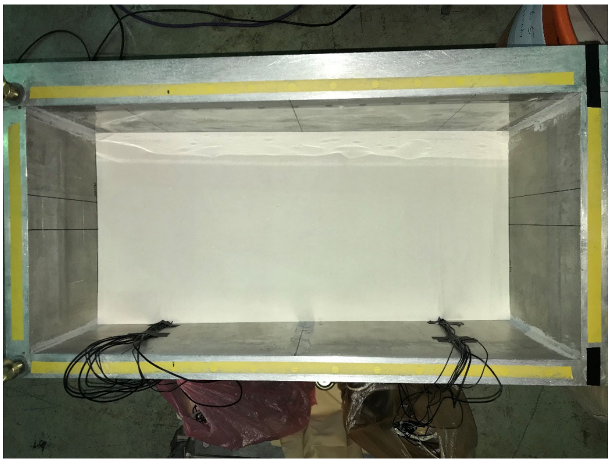

(a) Top view of dry model

(b) Curved surface

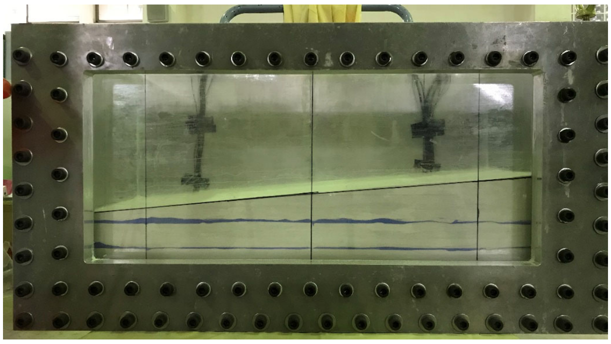

(c) Side view of dry model

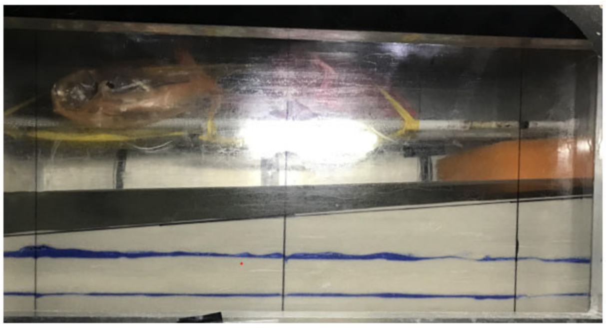

(d) Side view of saturated model

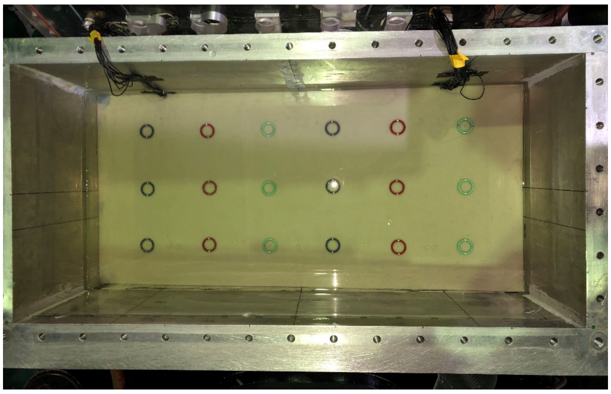

(e) Top view of saturated model

Figure 2-1 Model A photos before test

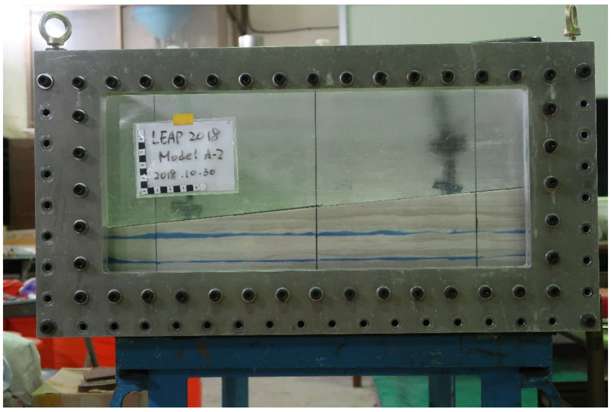

(a) Side view

(b) Side view before profile cutting

(c) Profile cutting for spaghettis

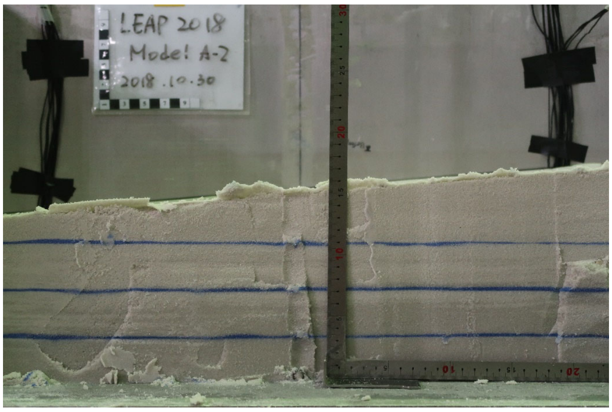

(d) Profile cutting for middle array pore pressure transducers

Figure 2-2 Model A photos after test

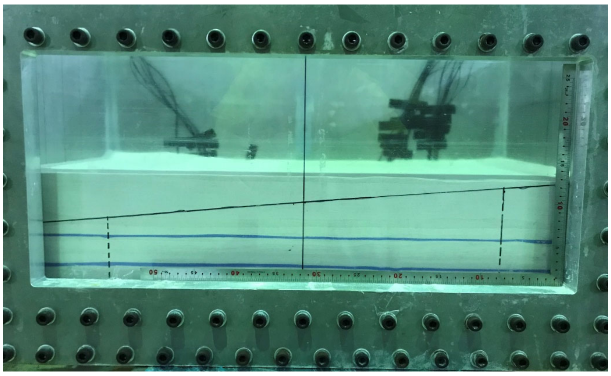

(a) Side view of dry model

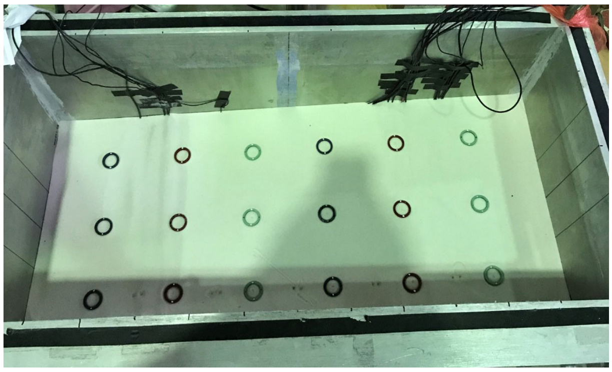

(b) Top view of dry model

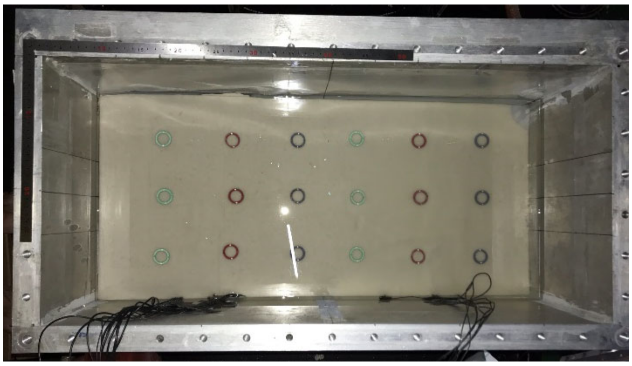

(c) Top view of saturated model

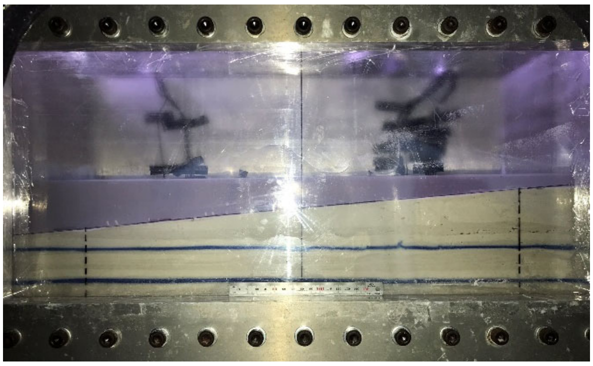

(d) Side view of saturated model

Figure 2-3 Model B profile before test

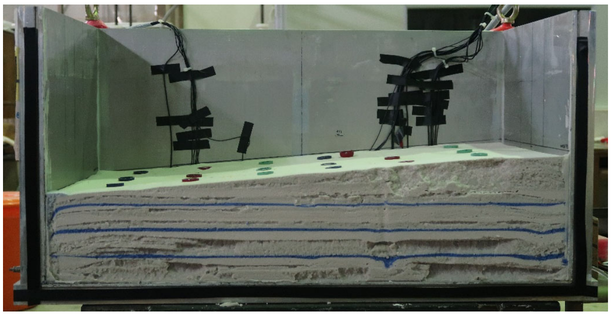

(a) Side view before profile cutting

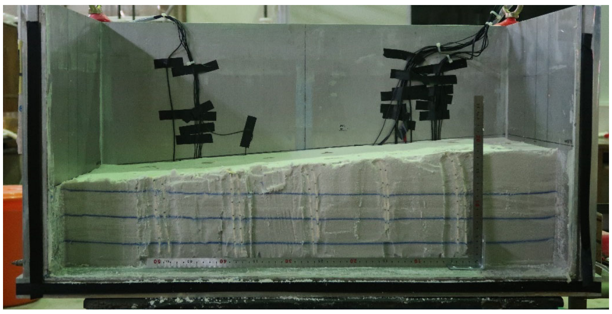

(b) Profile cutting for spaghetti

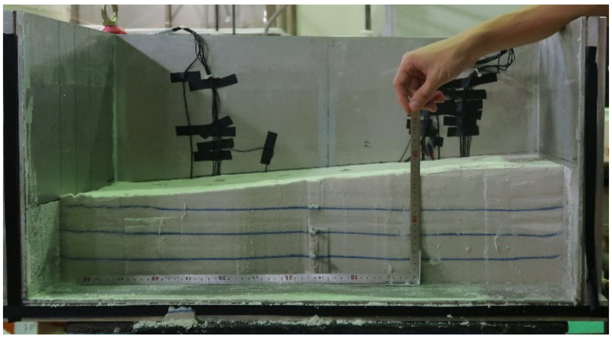

(c) Profile cutting for middle array pore pressure transducers

Figure 2-4 Model B photos after test

3. Comparison between model A and model B

Comparison (e.g., achieved PGA, EPWP, and surface displacements) between Model A and Model B tests (if they were completed). Discussion on the GSL and issues in the application of the GSL in practice.

The positions of sensors and the direction of positive acceleration are shown at Figure 3-1. The positive acceleration is toward upslope direction, conversely, the negative acceleration is toward downslope direction. This is the definition of the direction of results in this paper, and all of the results in this paper are presented in prototype scale.

3.1 Acceleration response

Figure 3-2 is the acceleration time histories of destructive motion 1 in model A and model B. The acceleration is expressed in prototype scale by taking scaling factor of 1/26 (η=26) in model A and 1/13 (η=13) in model B. The time histories indicate that the acceleration response of both models are very consistent, except the amplitude of spike signal at the surface layer is different.

3.2 EPWP behavior

Figure 3-3 shows the excess pore water pressure exceeding behavior during destructive motion 1 in model A and model B. The EPWP is expressed in prototype scale by taking scaling factor of 1 (μ=1) in model A and 2 (μ=2) in model B. Although the data lost at some locations, the result shows that both of the magnitude and exceeding behavior are very consistent at P2, P4 and P8. Figure 3-4 shows the EPWP dissipation behavior. We could observe that the dissipation time is slightly different at P2. This is affected by the viscosity of fluid.

3.3 Surface displacement

The surface displacement and settlement are expressed in prototype scale by taking scaling factor of 26 ($\mu^{1.5}\eta=1^{1.5}\times26$) in model A and 36.77 ($\mu^{1.5}\eta=2^{1.5}\times13$) in model B. Figure 3-5 shows the displacement vector of each marker. The maximum displacement happens at middle slope in model A but at downslope in model B. There is lower consistency of surface displacement behavior, both of magnitude and direction, between each model. Figure 3-6 shows the settlement of all markers. The maximum settlement happens at number 1 marker location (upslope), and maximum upheave induced by accumulation of upslope soil happens at number 6 maker location (downslope) in both models. However, the magnitude and the trend at middle slope are not consistent between each model.

3.4 Cone tip resistant

The distribution of q_c along the depth is plotted at Figure 3-8. The q_c is expressed in prototype scale by taking scaling factor of 1 (μ=1) in model A and 2 (μ=2) in model B. The value after destructive motion 1 is very consistent between model A and model

B. Before destructive motion 1, the value is very consistent at depth 0 m to 1.5 m, but the value is different at depth over 1.5 m. The difference of q_c may be influenced by the speed of penetration. The speed of penetration is not constant because the penetration force applied to CPT is applied by manually adjusting air pressure to cylinder.

3.5 Discussion on GSL

In general, the prototype of model B which the 1g virtual scaling factor (μ) is 2 seems can modeling the prototype of model A. However, the results of acceleration response and surface displacement behavior indicate the consistency of surface soil behavior is low. Therefore, more experiments are needed to validate GSL.

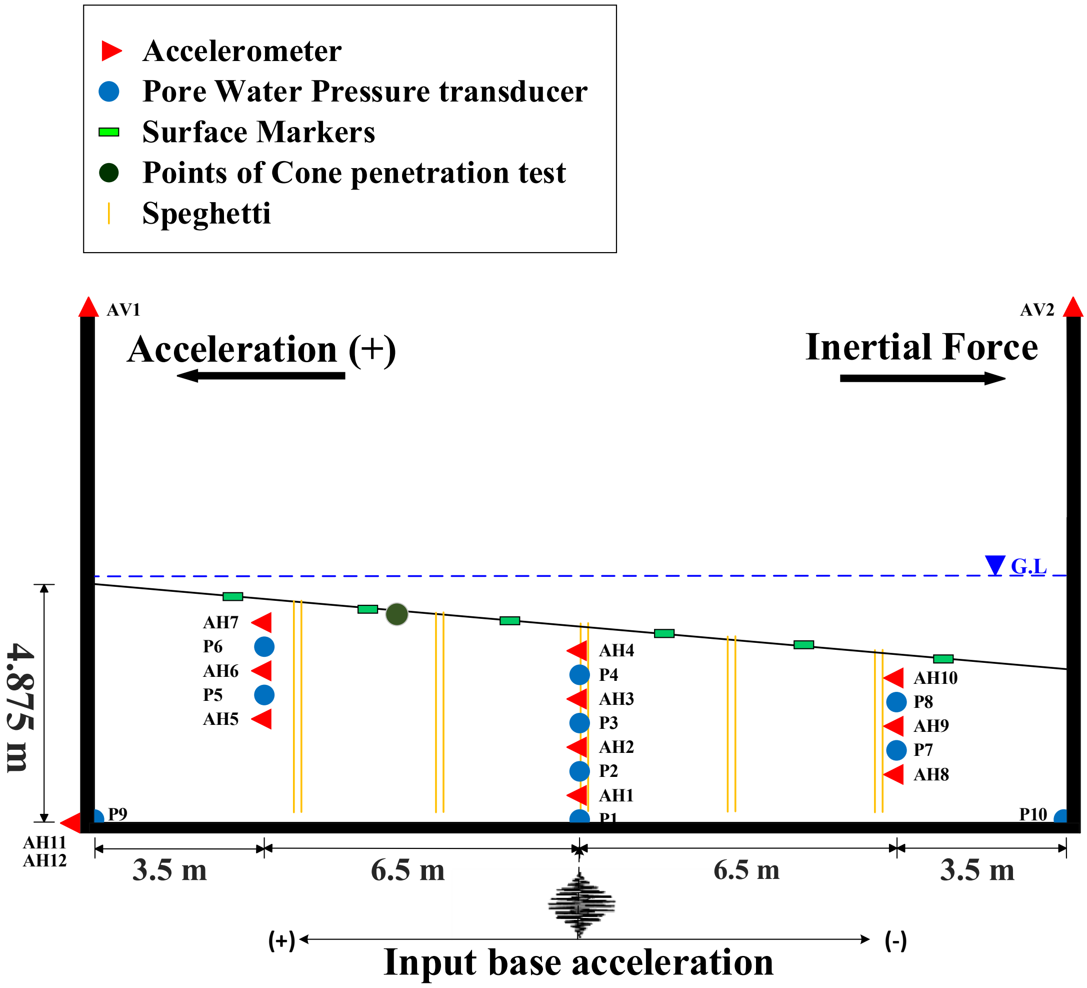

Figure 3-1 Model arrangement and direction definition of NCU models

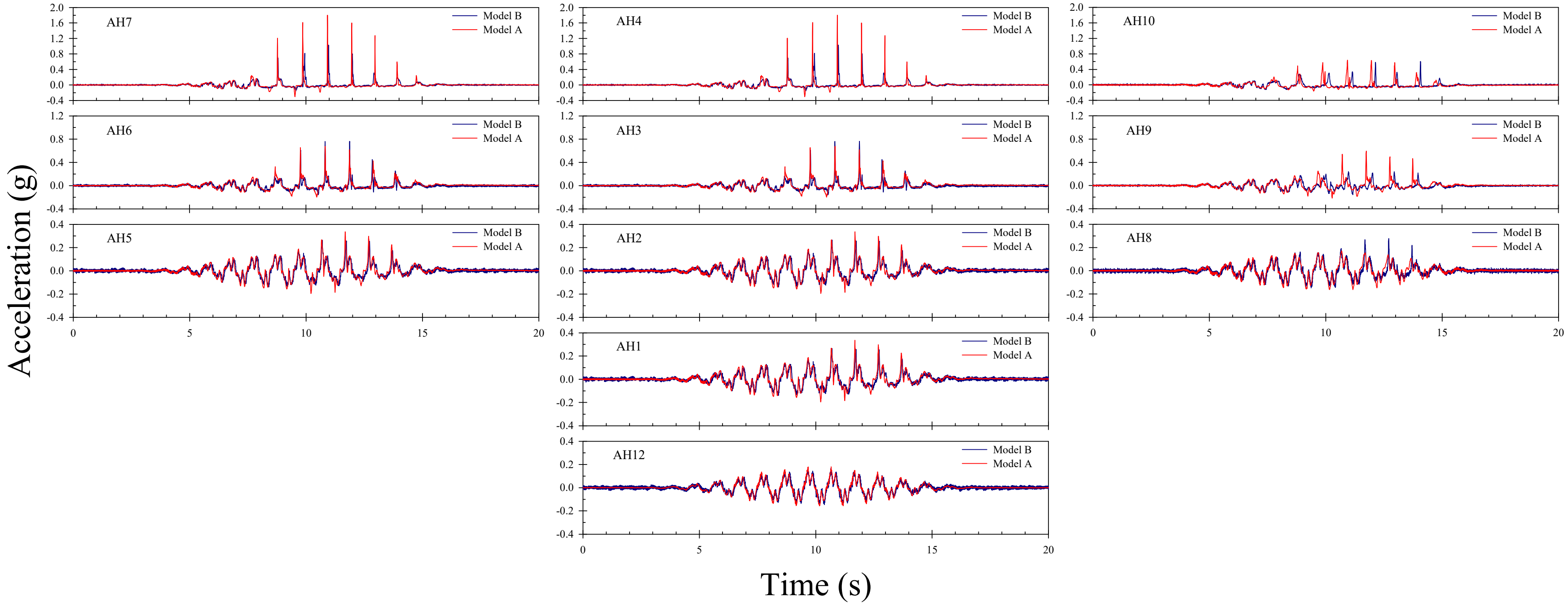

Figure 3-2 Acceleration time histories of main shaking (s2)

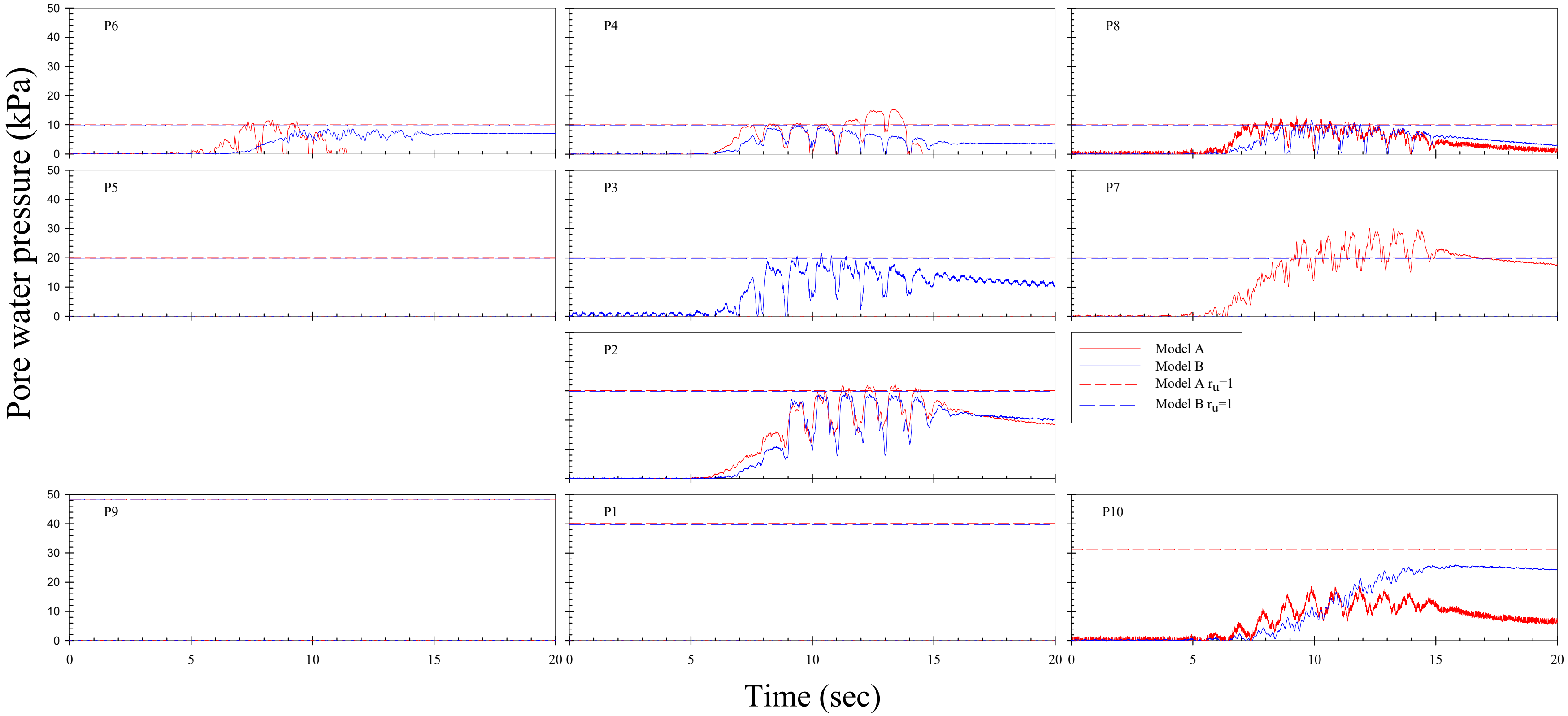

Figure 3-3 Excess pore water pressure time histories (20 seconds) of main shaking (s2)

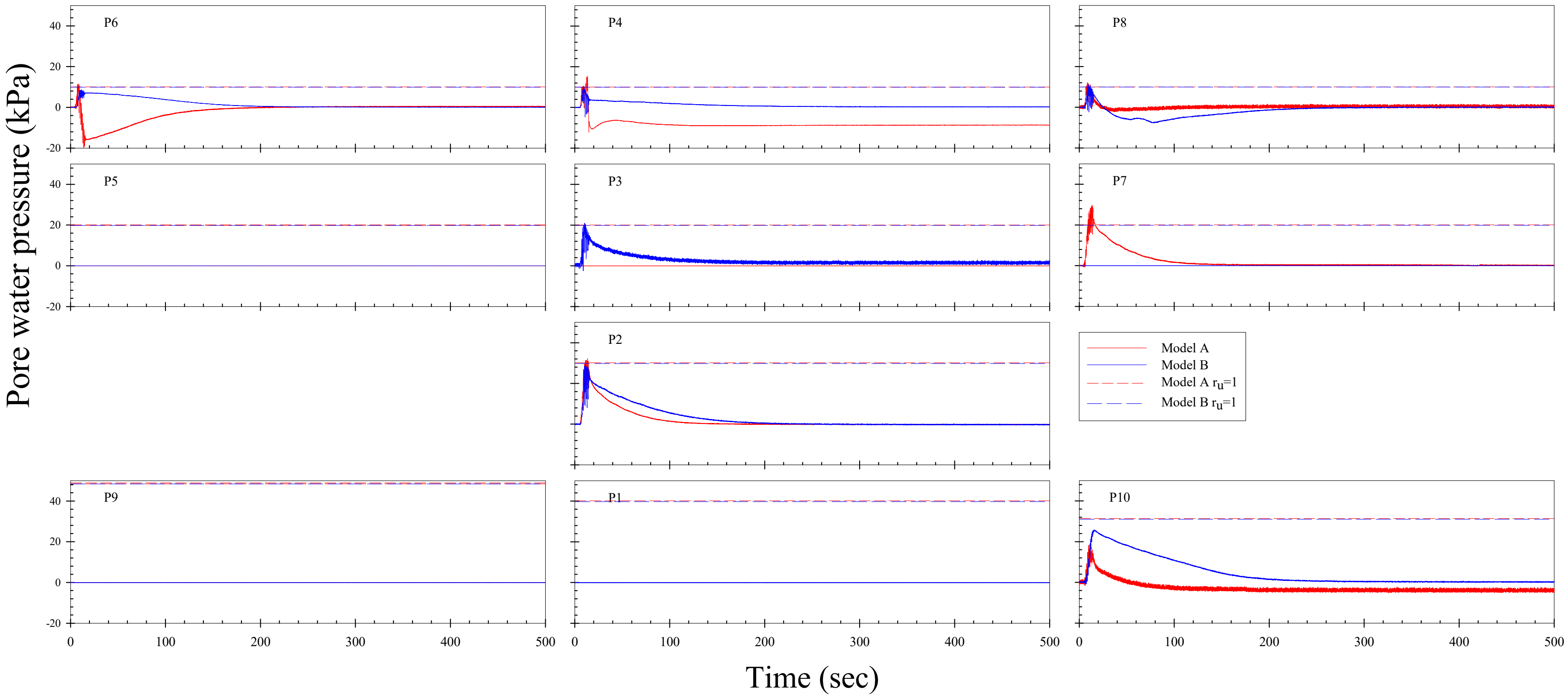

Figure 3-4 Excess pore water pressure time histories (500 seconds) of main shaking (s2)

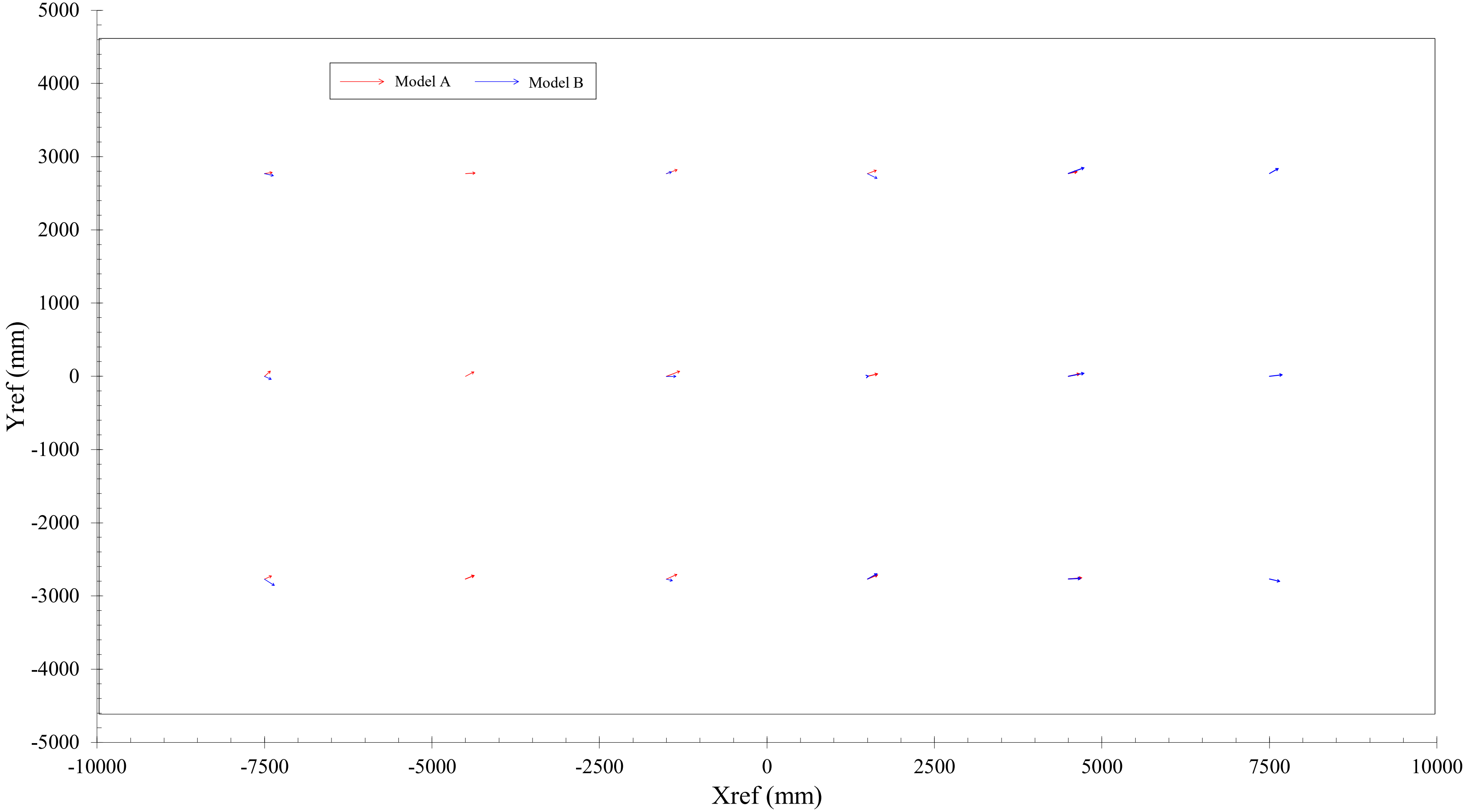

Figure 3-5 Displacement of surface markers

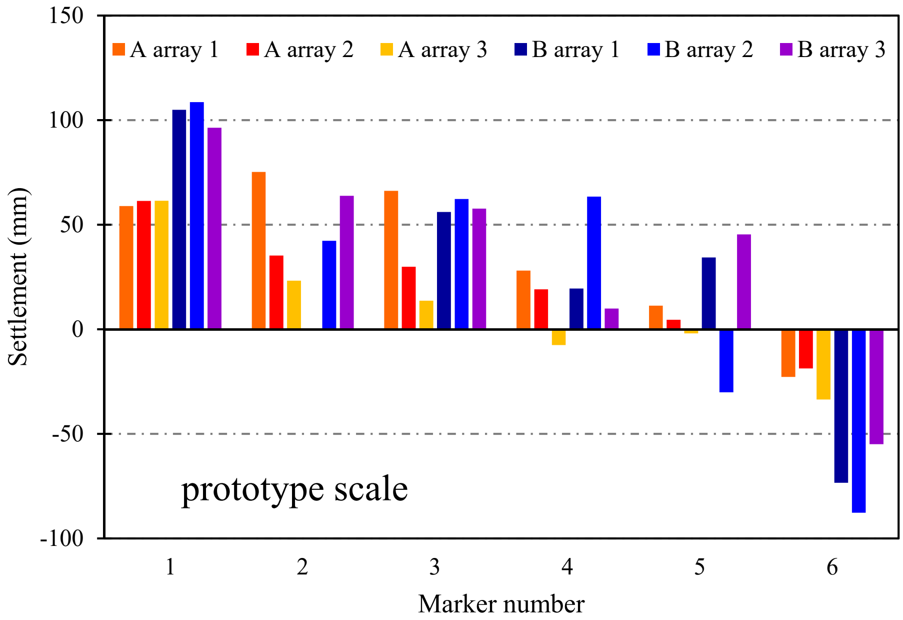

Figure 3-6 Settlement of all markers

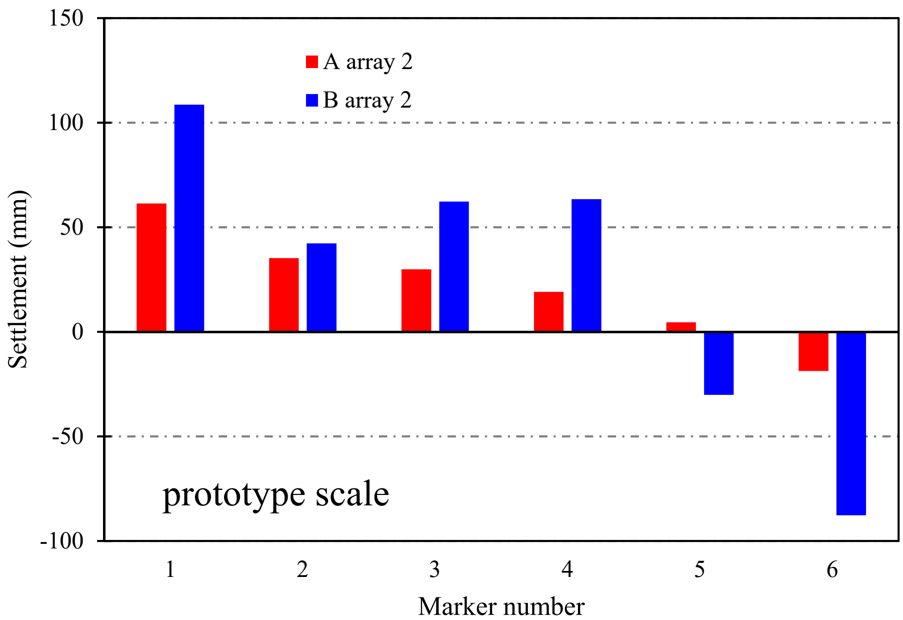

Figure 3-7 Settlement of array 2 markers

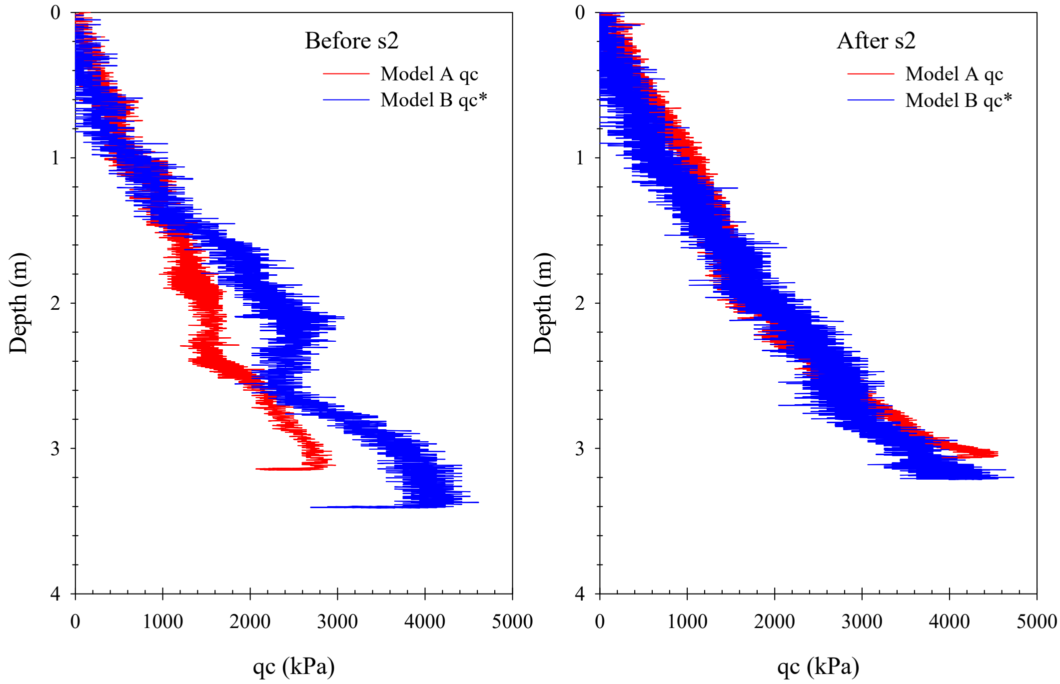

Figure 3-8 Cone tip resistance (q_c) distribution along the depth

4. Pre-shaking analysis and spaghetti deformation

Explanation of nuances and unique features of your experiments, especially the features that are not explained in the excel data templates previously submitted and clarification of information submitted in excel templates.

4.1 Shear velocity

Pre-shaking technique is to detect the shear velocity and predominant frequency of soil strata by inputting a non-destructive motion which is a 3Hz, PBA = 0.04 g, 1 cycle sine wave. The amplitude and duration of motion are small and short enough so that it would only exceed little or even no excess pore water pressure.

$$v_s = \frac{L}{\Delta t} \qquad (4\text{-}1)$$

where v_s = shear velocity (m/s), L = distance (m), Δt = time difference (s).

Shear velocity of soil strata is determined by Formula (4-1). The arrival time of wave is got from each accelerometer time history, afterward, the difference arrival time between each accelerometer can be determined. Moreover, the distance between each accelerometer is given. The shear velocity of soil strata is finally figured out. The results are shown in Figure 4-1. The average shear velocity is averaged out the shear velocity of 3 arrays. In model A case, the average shear velocity is 367 m/s and 520 m/s before and after destructive motion (s2), respectively. In model B case, the average shear velocity is 296 m/s and 340 m/s before and after destructive motion (s2), respectively. The shear velocity of soil strata is related to the density of soil strata. Denser soil has larger shear velocity, and the density of model A is larger than the density of model B. In addition, the density of soil strata after destructive motion (s2) is supposed to be larger than the density of soil strata before destructive motion (s2). Therefore, the results are reasonable.

4.2 Predominate frequency

Transform the free vibration signal of pre-shaking acceleration time histories to frequency domain from time domain via fast Fourier transform. Figure 4-2 shows the Fourier spectra of acceleration time histories in s1 and s3. From Fourier spectra, the predominant frequency of soil strata in model A is 5.25 Hz and in model B is 5.5 Hz. In addition, the frequency of free vibration can be estimated from acceleration time histories. The estimated frequency of free vibration is approximately at the range of 5 to 6 Hz.

4.3 Spaghetti deformation

The spaghetti were penetrated into soil strata during model preparation. The spaghetti were supposed to deform with the soil strata, therefore, the deformation behavior of soil strata can be estimated by the displacement of spaghetti. The soil strata profile is got by cutting model after test. The horizontal displacement of spaghetti along the depth (Figure 4-5) is determined via image digitalized tool from the soil profile. The result indicates the horizontal displacement of soil decrease with increasing depth in both models. But the displacement in model B is larger than in model A. The displacement may be influenced by the initial density or the error of GSL.

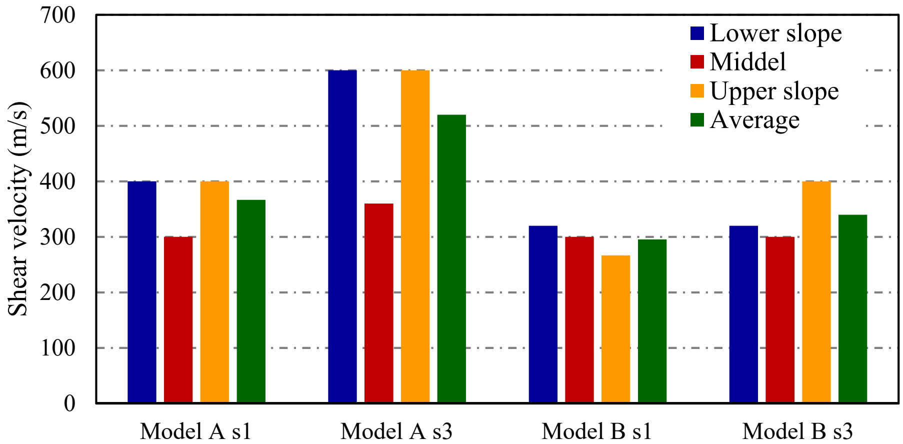

Figure 4-1 Shear velocity of soil strata before and after main shaking

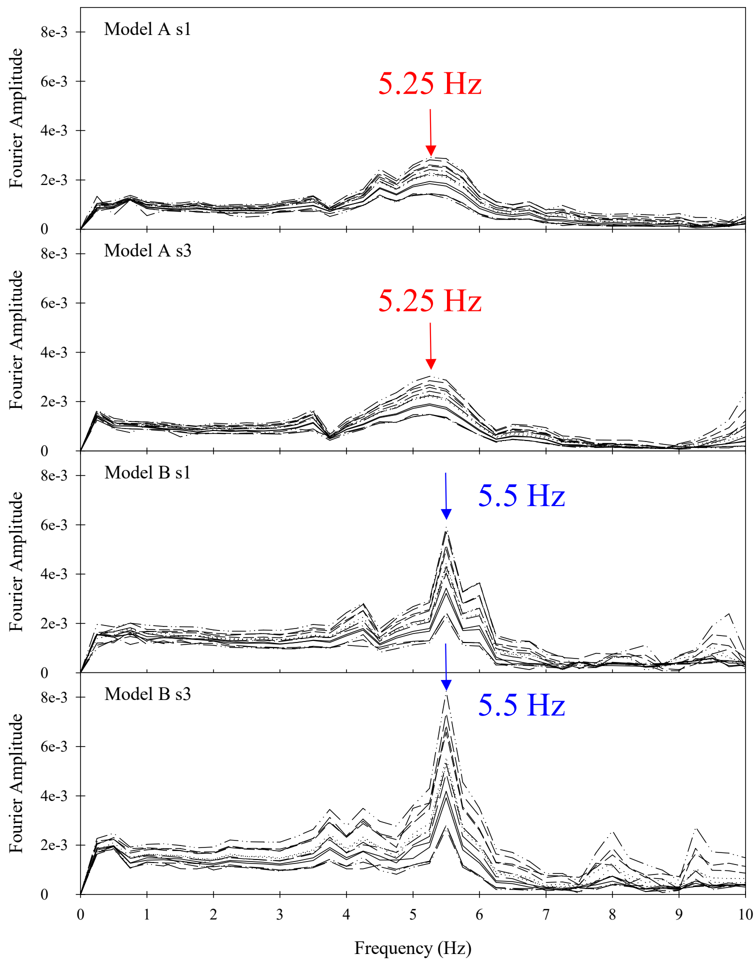

Figure 4-2 Fourier spectra of acceleration time histories in s1 and s3

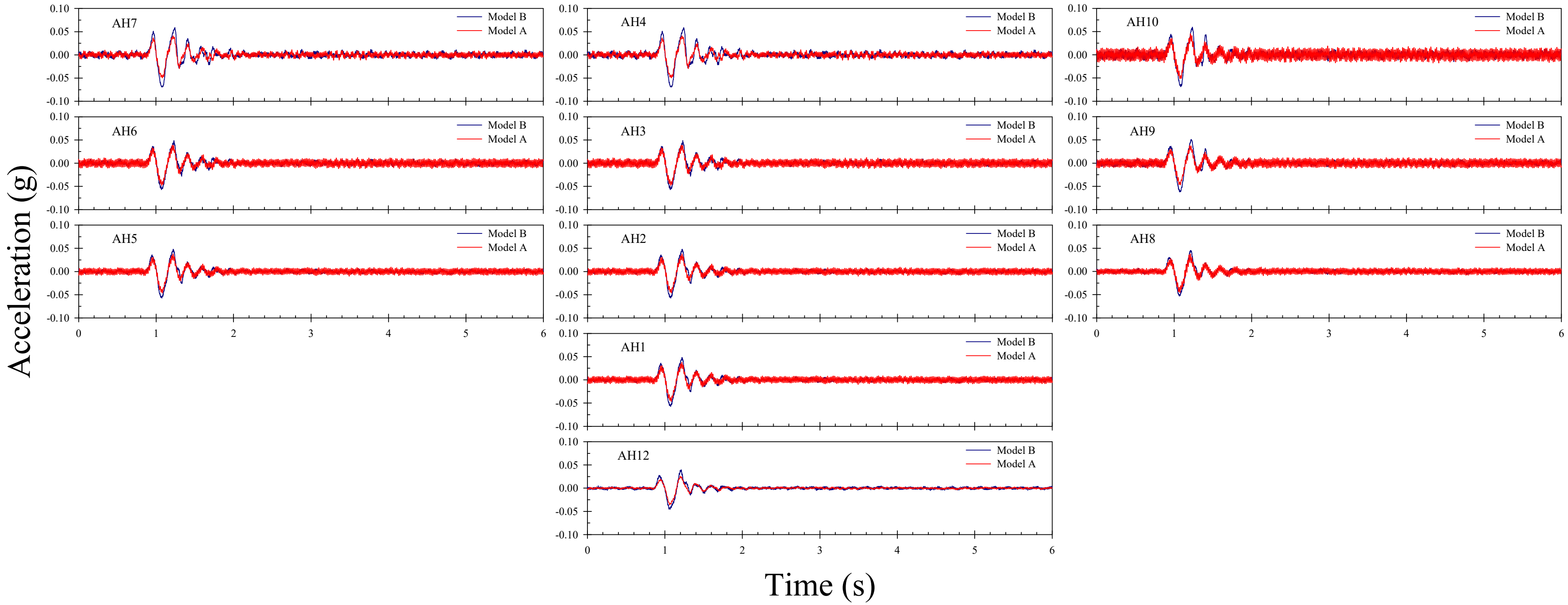

Figure 4-3 Acceleration time histories of s1 (pre-shaking before main shaking)

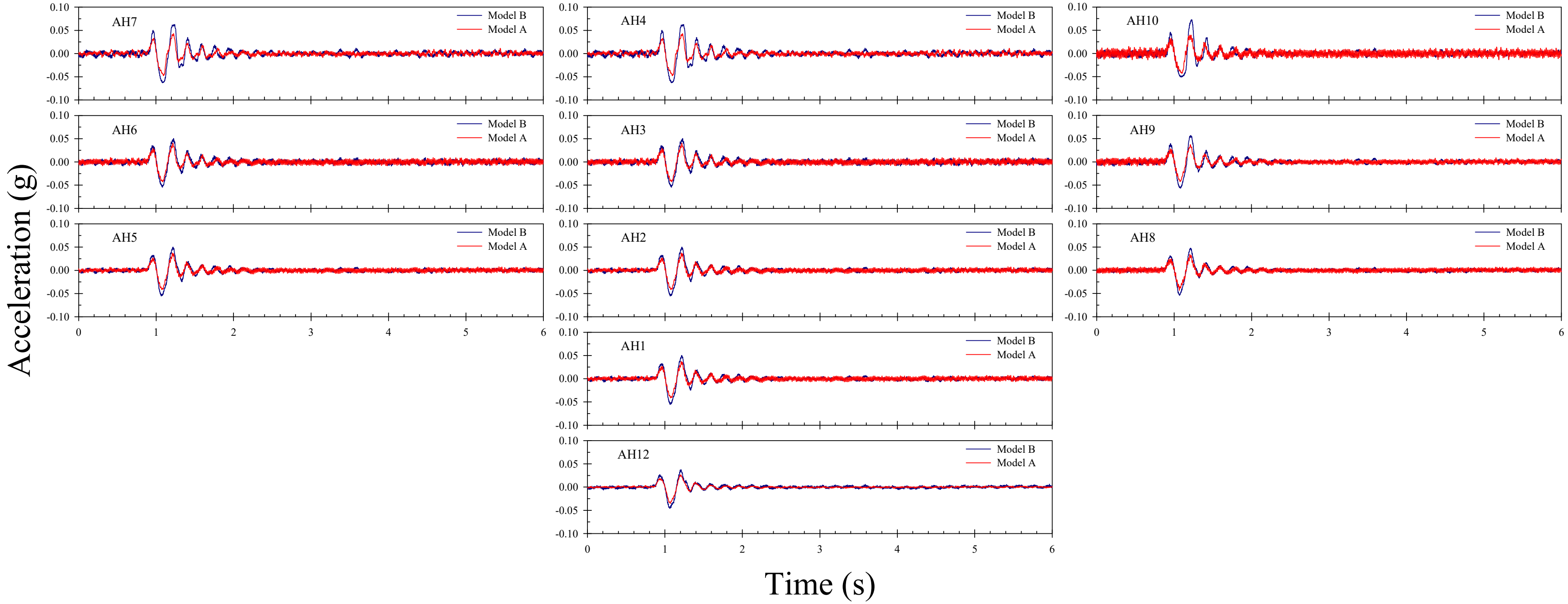

Figure 4-4 Acceleration time histories of s3 (pre-shaking after main shaking)

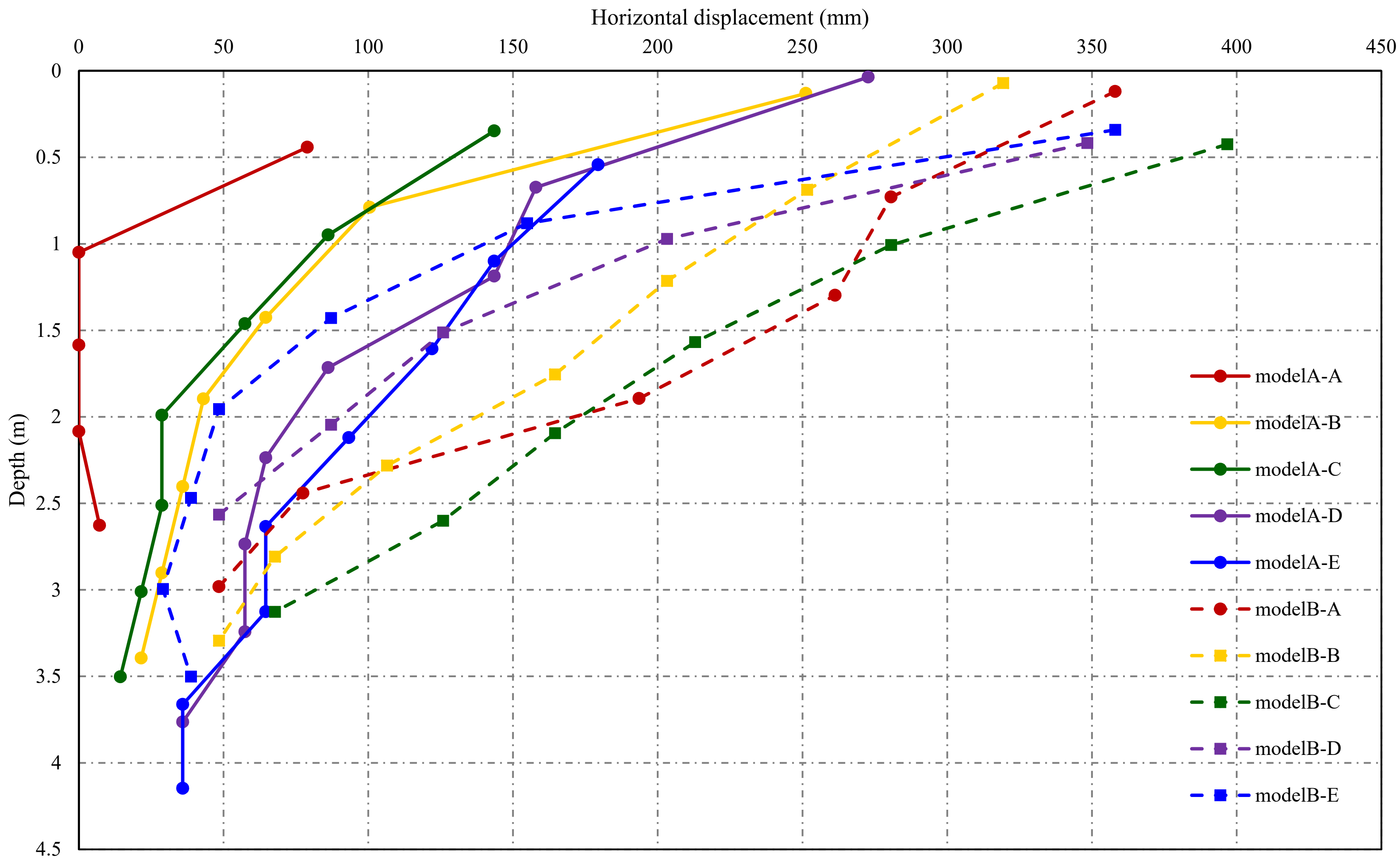

Figure 4-5 Displacement of spaghetti along the depth after test

5. LEAP-UCD-2017 vs. LEAP-ASIA-2019

Comparison of your experimental results to the trend of data observed in LEAP-UCD-2017 and LEAP-ASIA-2019. If your results do not follow the trend of the existing body of centrifuge test data, can the difference be explained by uncertainties or errors in the existing trend or your experiments?

Figure 5-1 and 5-2 are the acceleration and EPWP time histories of NCU models in LEAP-UCD-2017. The density of models and the PBA of input motions are different with NCU models in LEAP-ASIA-2019. The density of models is 1651, 1653, 1653 kg/cm^3 corresponding to NCU 1, NCU 2, NCU 3 in LEAP-USD-2017. The achieved PBA of motion is 0.265, 0.221, 0.185 g corresponding to NCU 1-m1, NCU 2-m1, NCU 3-m3. Although density and PBA of models in LEAP-UCD-2017 are denser and larger than models in LEAP-ASIA-2019, the trend of results in both projects is similar.

6. After-action review

Description of improvements in the data reporting excel template and in the experiment specifications that could be addressed in future LEAP exercises

The AAR for NCU tests in LEAP-ASIA-2019 is described below.

(1) There are many data loss in EPWP time histories because there was not enough good performance of PPT (pore pressure transducer) when the LEAP-ASIA-2019 models were carried out. We are going to buy new FBG (fiber Bragg Grating) PPT now. The desirable performance of PPT can be achieved from NCU models in the future.

(2) The CPTs were manually controlled by force control system when the LEAP-ASIA-2019 models were carried out. We are going to design and make an automatic displacement control system for CPT. The penetration rate will be constant and conform to the requirements of LEAP experiment.

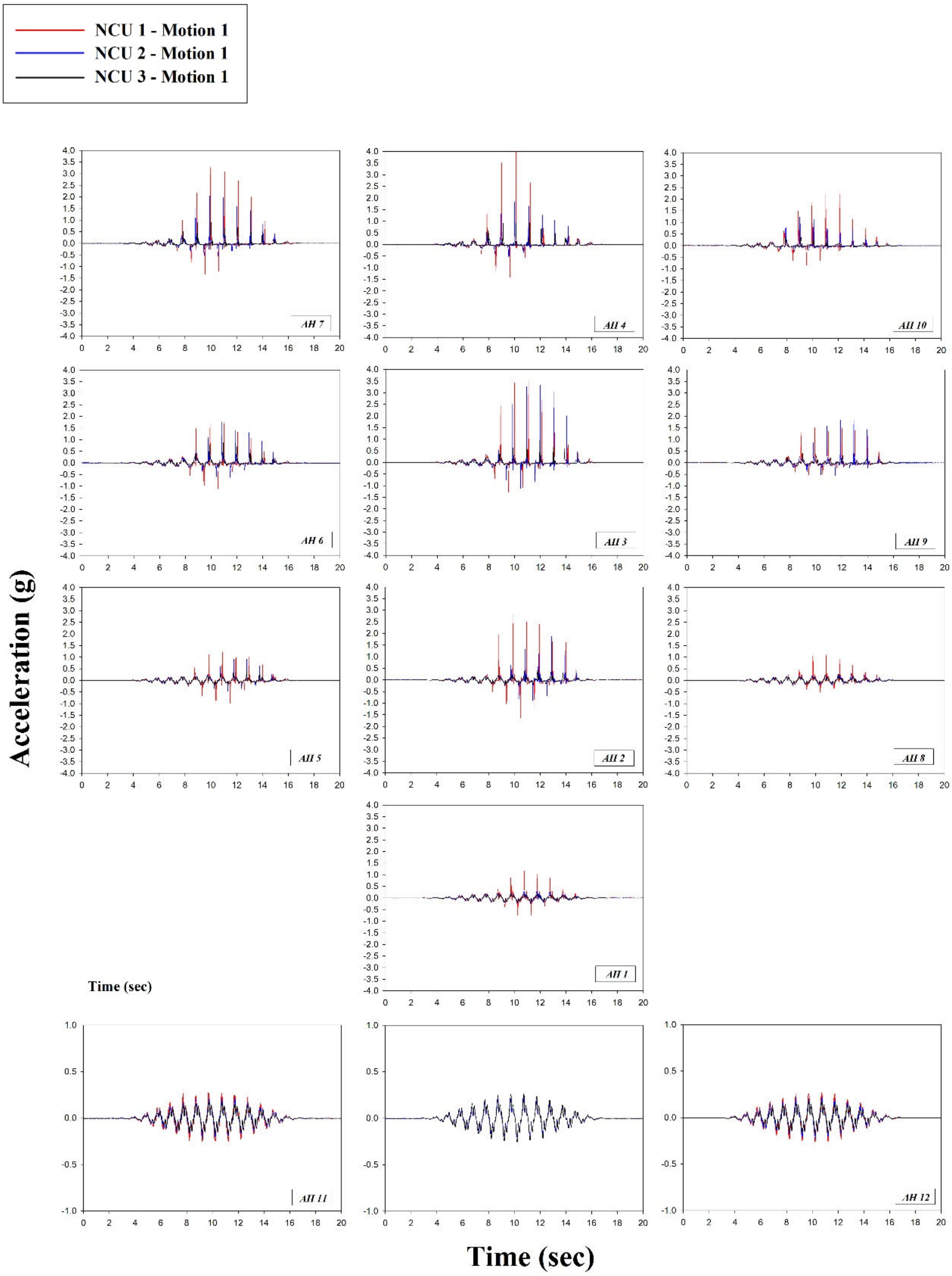

Figure 5-1 The time histories of acceleration for NCU1-m1, NCU2-m1 and NCU3-m1 in LEAP-UCD-2017

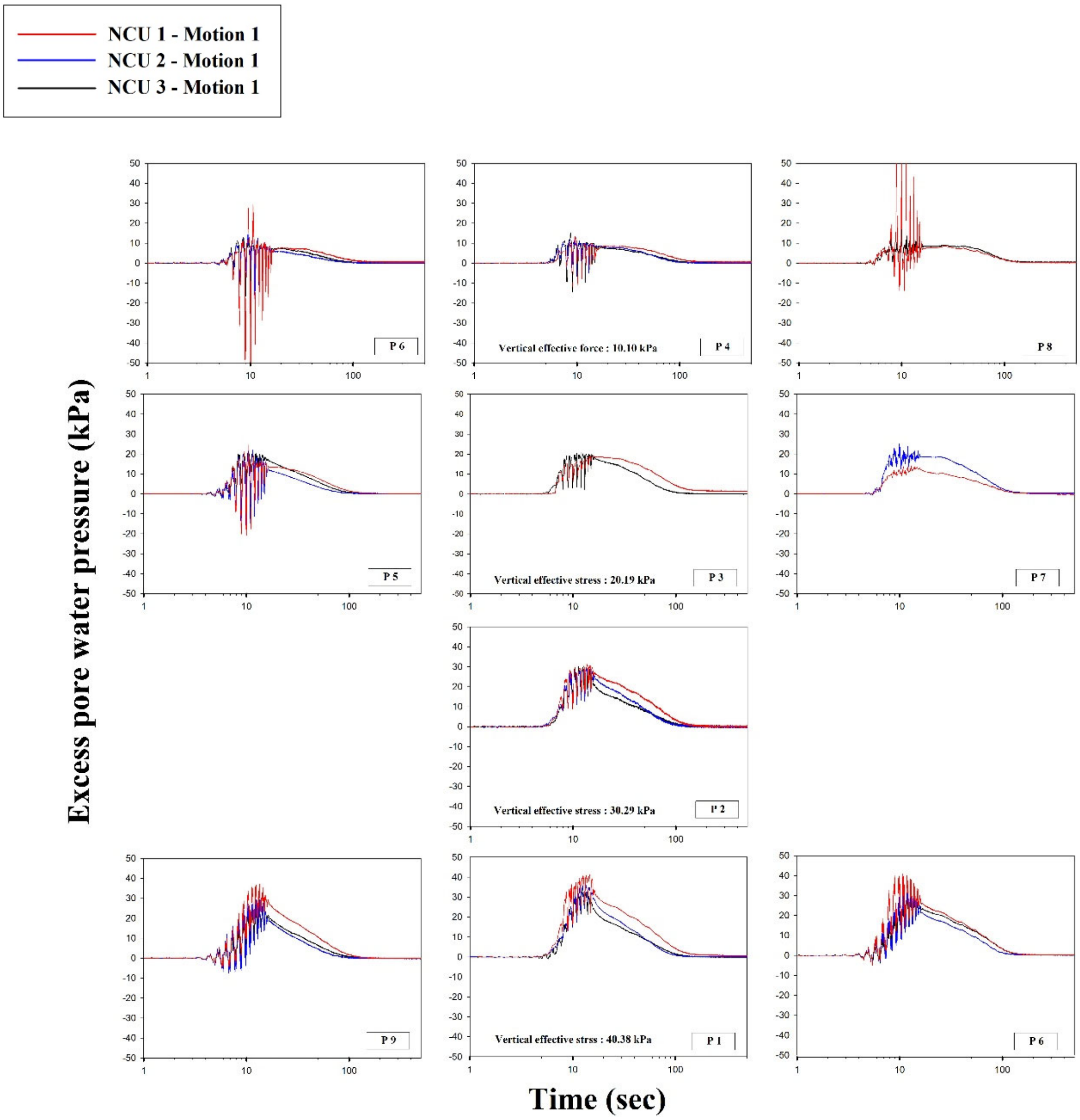

Figure 5-2 The time histories of pore water pressure for NCU1-m1, NCU2-m1 and NCU3-m1 in LEAP-UCD-2017